Supporting Information

Magnetically Induced Anisotropic Orientation of Graphene Oxide Locked by *in Situ* Hydrogelation

Linlin Wu,[1] Masataka Ohtani,[2] Masaki Takata,[3] Akinori Saeki,[4] Shu Seki,[4] Yasuhiro Ishida,[2]* and Takuzo Aida[1,2]

[1] *Department of Chemistry and Biotechnology, School of Engineering, The University of Tokyo, 7-3-1 Hongo, Bunkyo-ku, Tokyo 113-8656, Japan*

[2] *RIKEN Center for Emergent Matter Science, 2-1 Hirosawa, Wako, Saitama 351-0198, Japan*

[3] *RIKEN SPring-8 Center, 1-1-1 Kouto, Sayo, Hyogo 679-5198, Japan*

[4] *Department of Applied Chemistry, Osaka University, 2-1 Yamadaoka, Suita, Osaka 565-0871, Japan*

Table of Contents

1. Estimation of Orientation Order Parameter

The orientation order parameter (S) was estimated using the azimuthal angle plots obtained from the 2D small-angle X-ray scattering (2D SAXS) images.[S1,S2] Scattering in 2D SAXS images at q = 0.08–0.44 nm^{-1} were integrated for every 5° in azimuthal angle by using a Rigaku model R-AXIS Display software. The S values range between 0 and 1, where the former corresponds to an isotropic structure and the latter corresponds to perfect orientation along the director. A Maier-Saupe distribution function (eq. 1) was used to fit the azimuthal angle plots[S3]

$$I = I_0 + A\exp\left(\alpha\cos^2\left(\varphi - \varphi_0\right)\right) \quad (1)$$

where I_0 denotes the free baseline intensity, φ_0 is the azimuth at the position of the maximal intensity, φ is the azimuth, and α is the parameter that determines the width of the distribution. After the curve fitting of this function to the azimuthal angle plot, parameters I_0, A, and α were obtained. The orientation order parameter S was determined using the following equation[S2]

$$S = \frac{\int_{-1}^{1} P_2(\cos\varphi)\exp\left(\alpha\cos^2\varphi\right)d\cos\varphi}{\int_{-1}^{1}\exp\left(\alpha\cos^2\varphi\right)d\cos\varphi} \quad (2)$$

where the function $P_2(\cos\varphi)$ is the second-order Legendre polynomial of cos φ, often referred to as the Hermans orientation function.

$$P_2(\cos\varphi) = \frac{1}{2}(3\cos^2\varphi - 1) \quad (3)$$

2. AFM and SEM Images of GO

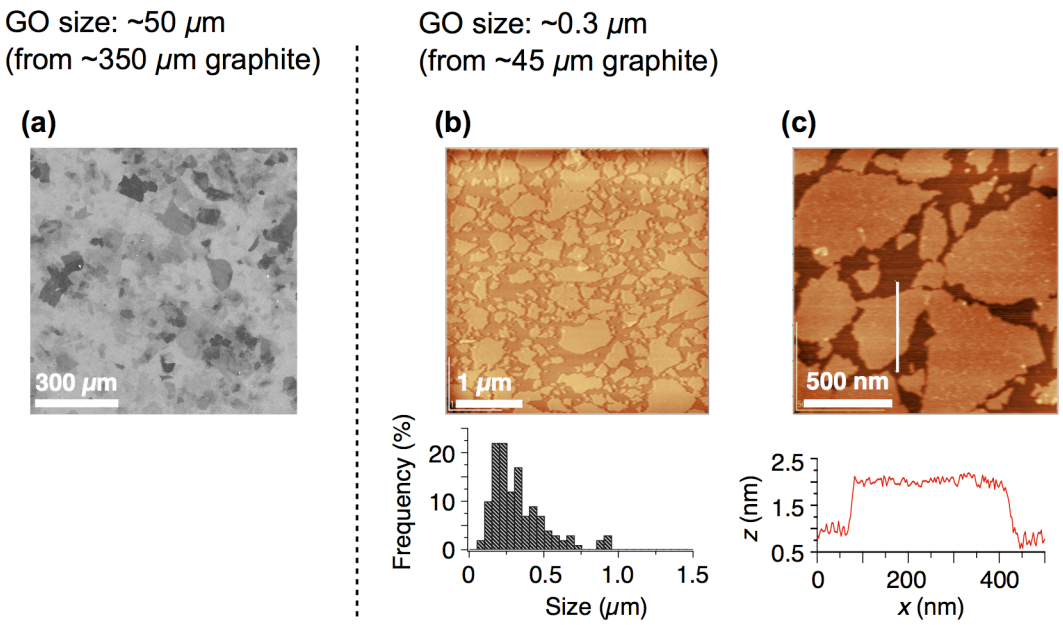

Figure S1. (a) SEM image of GO prepared from expandable graphite with the averaged size of ~350 μm. (b,c) AFM images of GO prepared from graphite powder with the averaged size of ~45 μm. Measurements were performed under tapping mode (phase imaging) in air with standard Si probes. Samples were prepared by spin-coating aqueous GO dispersions onto mica.

3. FT-IR Spectra of GO and Precursory Graphite

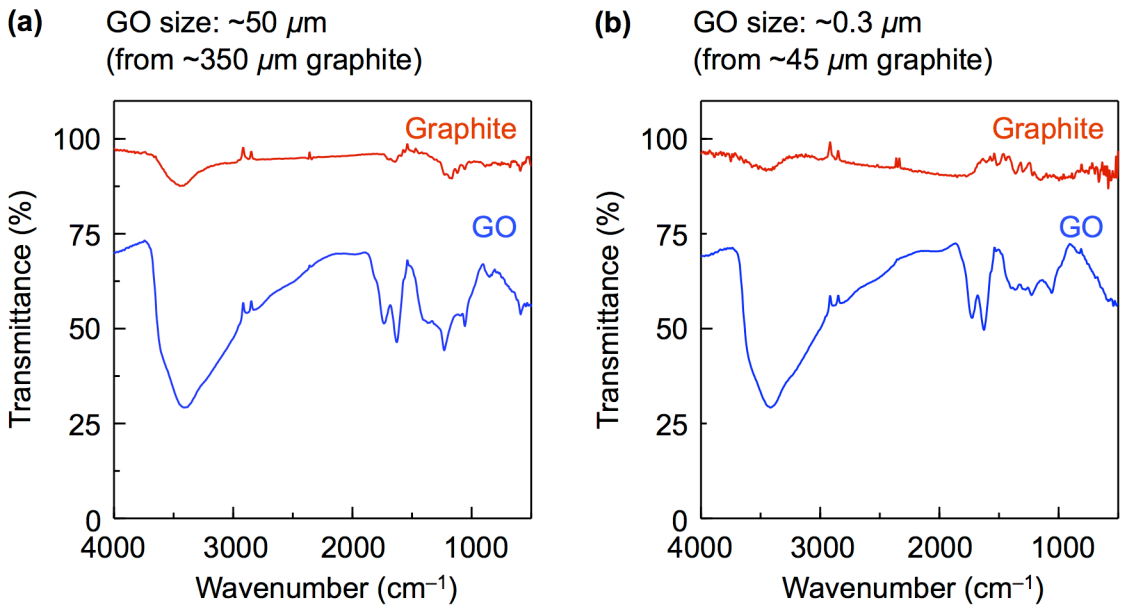

Figure S2. FT-IR spectra of GO (blue curve) and precursor graphite (red curve). Averaged sizes of GO/precursor graphite: (a) ~350/~50 μm and (b) ~45/~0.3 μm.

4. Raman Spectra of GO and Precursory Graphite

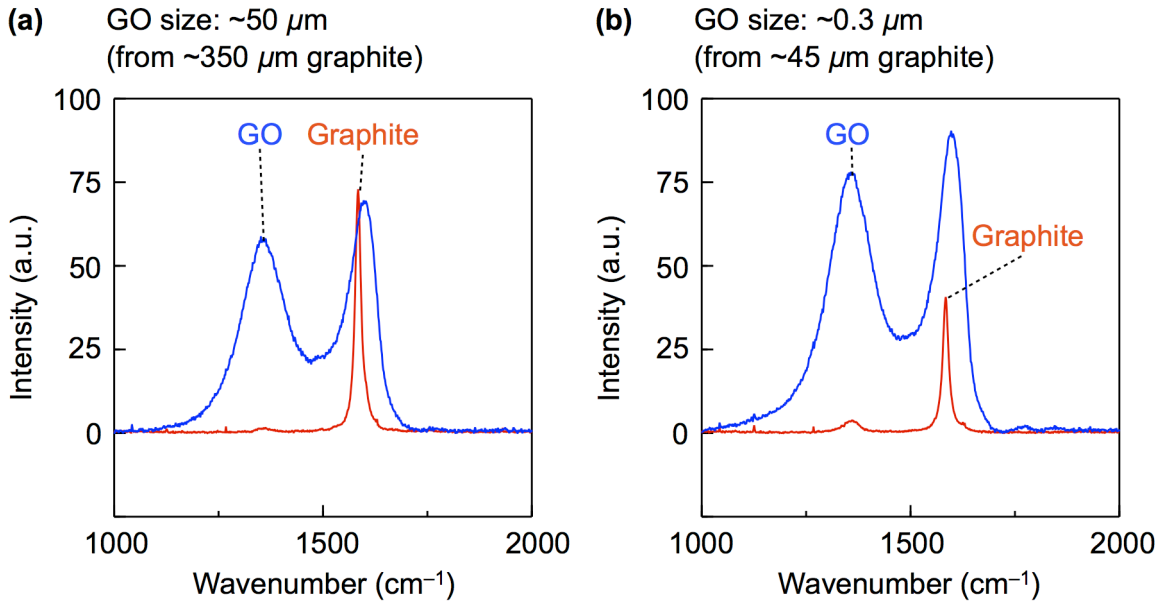

Figure S3. Raman spectra of GO (blue curve) and precursor graphite (red curve). Averaged sizes of GO/precursor graphite: (a) ~50/~350 μm and (b) ~0.3/~45 μm.

5. Energy Dispersion X-Ray Spectra of GO

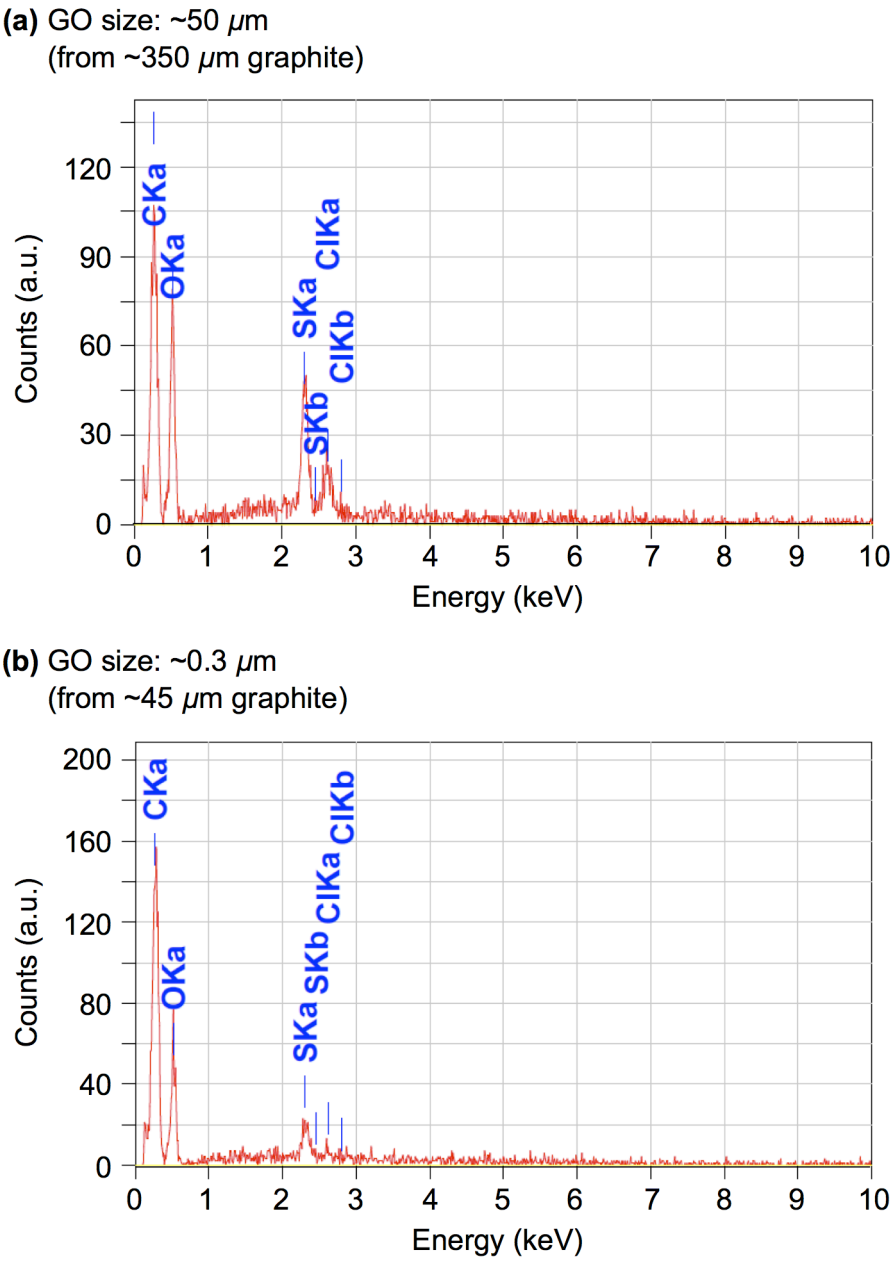

Figure S4. Energy dispersion X-ray spectra of GO samples. Averaged sizes of GO/precursor graphite: (a) ~50/~350 μm and (b) ~0.3/~45 μm.

6. 2D SAXS Images of GO-Hybridized Hydrogels

6-1. Effects of Gravitational Field

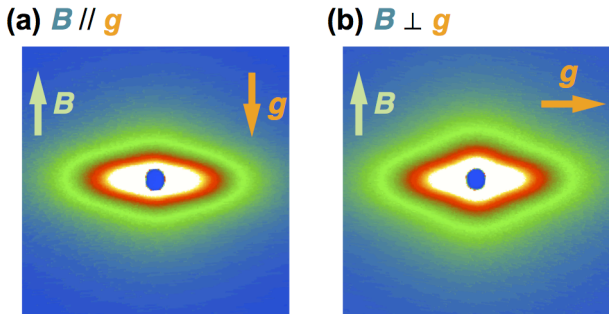

Figure S5. 2D-SAXS images of GO-hybridized hydrogels (GO/monomer/crosslinker = 0.20/3.0/0.16 wt%) prepared in a 10-T magnetic field directed (a) parallel and (b) orthogonal to the gravity. The hydrogels were exposed to an X-ray beam from the orthogonal direction to the magnetic field applied in the preparation of the GO-hybridized hydrogels. ***B***: magnetic field. ***g***: gravitational field.

6-2. Effects of Sample Shape Anisotropy

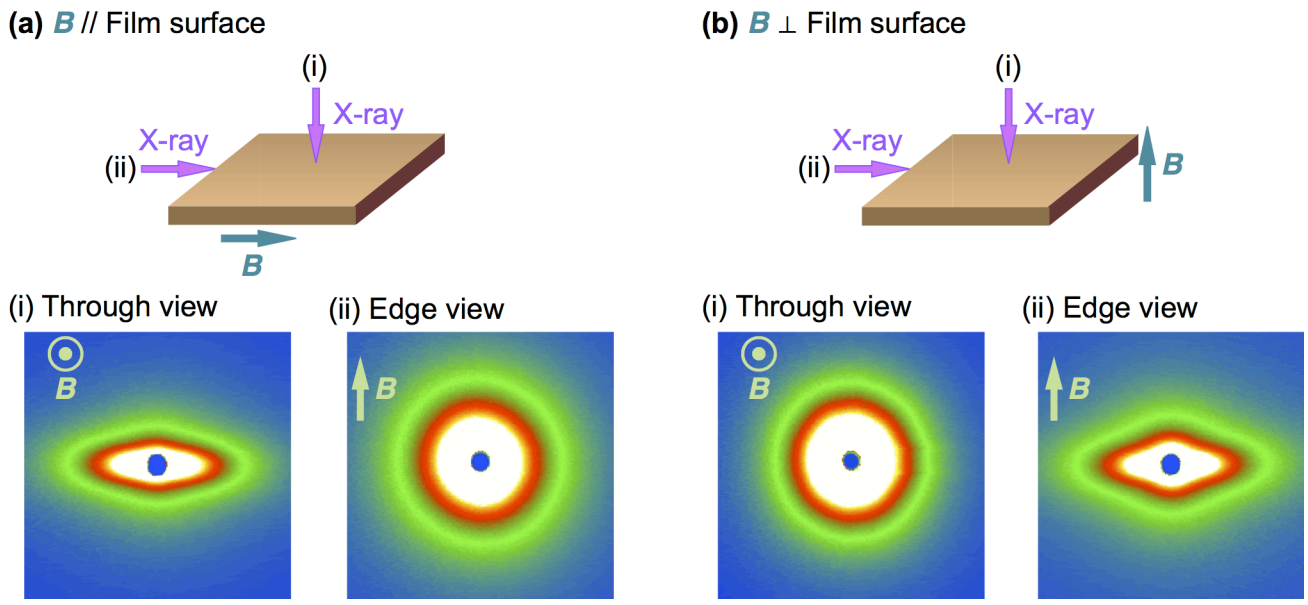

Figure S6. 2D-SAXS images of GO-hybridized hydrogel films (1-mm thick, 10-mm × 20-mm width, GO/monomer/crosslinker = 0.20/3.0/0.16 wt%) prepared in a 10-T magnetic field directed (a) parallel and (b) orthogonal to the film surface. The hydrogels were exposed to an X-ray beam from (i) the parallel and (ii) orthogonal directions to the film surface. In (a-ii), the X-ray was parallel to the to the magnetic field applied in the preparation of the GO-hybridized hydrogels.

6-3. Effects of Magnetic Field Intensity

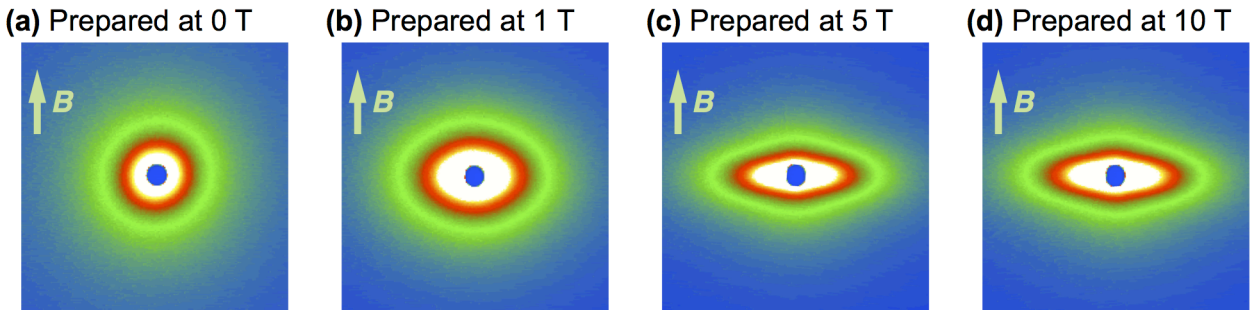

Figure S7. 2D-SAXS images of GO-hybridized hydrogels (GO/monomer/crosslinker = 0.20/3.0/0.16 wt%) prepared in a magnetic field with varying intensity: (a) 0, (b) 1, (c) 5, and (d) 10 T. The hydrogels were exposed to an X-ray beam from the orthogonal direction to the magnetic field applied in the preparation of the GO-hybridized hydrogels.

6.4. Effects of GO Concentration

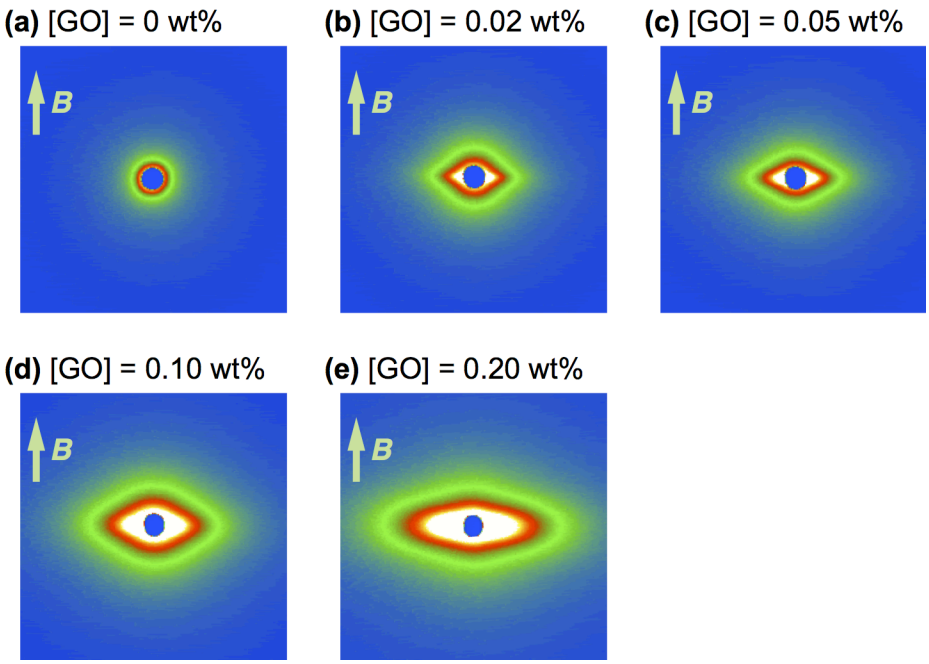

Figure S8. 2D-SAXS images of GO-hybridized hydrogels (monomer/crosslinker = 3.0/0.16 wt%, prepared in a 10-T magnetic field) with various GO concentrations: (a) 0, (b) 0.02, (c) 0.05, (d) 0.10, and (e) 0.20 wt%. The hydrogels were exposed to an X-ray beam from the orthogonal direction to the magnetic field applied in the preparation of the GO-free and GO-hybridized hydrogels.

6.5. Effects of GO Size

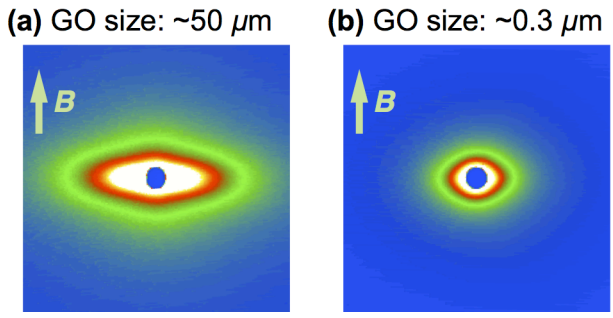

Figure S9. 2D-SAXS images of GO-hybridized hydrogels (GO/monomer/crosslinker = 0.10/3.0/0.16 wt%, prepared in a 10-T magnetic field) with averaged GO sizes of (a) ~50 and (b) ~0.3 μm. The hydrogels were exposed to an X-ray beam from the orthogonal direction to the magnetic field applied in the preparation of the GO-hybridized hydrogels.

7. POM Images of GO-Hybridized Hydrogels after Magnetic Treatment

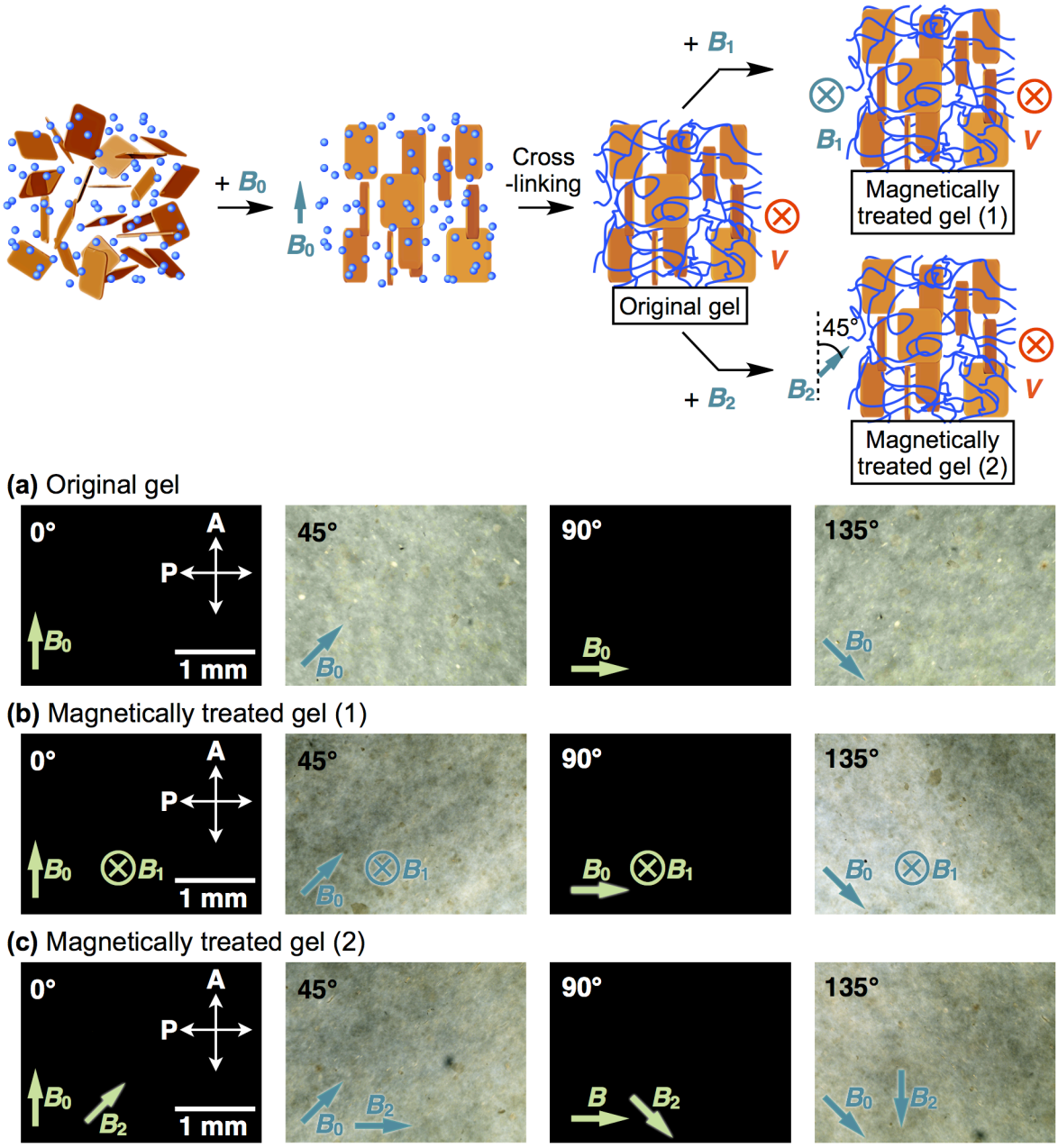

Figure S10. POM images of GO-hybridized hydrogels (1-mm thick, GO/monomer/crosslinker = 0.20/3.0/0.16 wt%, prepared in a 10-T magnetic field [$\boldsymbol{B_0}$]), where the viewing direction ($\boldsymbol{V}$) was orthogonal to $\boldsymbol{B_0}$: (a) original and (b,c) after being treated at 20 °C for 48 h with 10-T magnetic fields directed parallel (b; $\boldsymbol{B_1}$) and orthogonal (c; $\boldsymbol{B_2}$) to $\boldsymbol{V}$. In (c), the crossing angle between $\boldsymbol{B_0}$ and $\boldsymbol{B_2}$ was 45°. The images were obtained by varying the angle between the direction of the analyzer and that of the applied magnetic field (0°, 45°, 90°, and 135°).

8. SEM Images of the Xerogels of GO-Hybridized Hydrogels

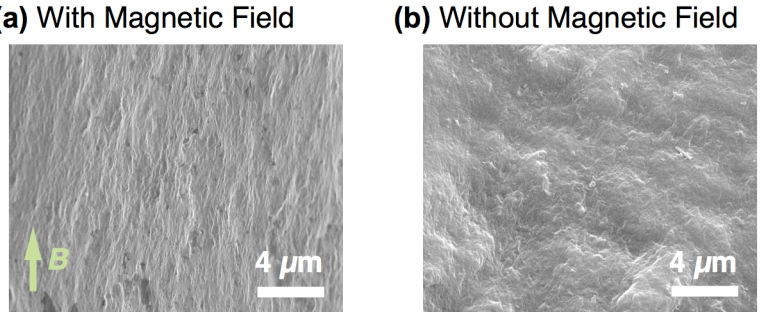

Figure S11. SEM images of the xerogels of GO-hybridized hydrogels (GO/monomer/crosslinker = 0.20/3.0/0.16 wt%) prepared (a) in a 10-T magnetic field and (b) without magnetic field.

9. POM Images of Aqueous GO Dispersions

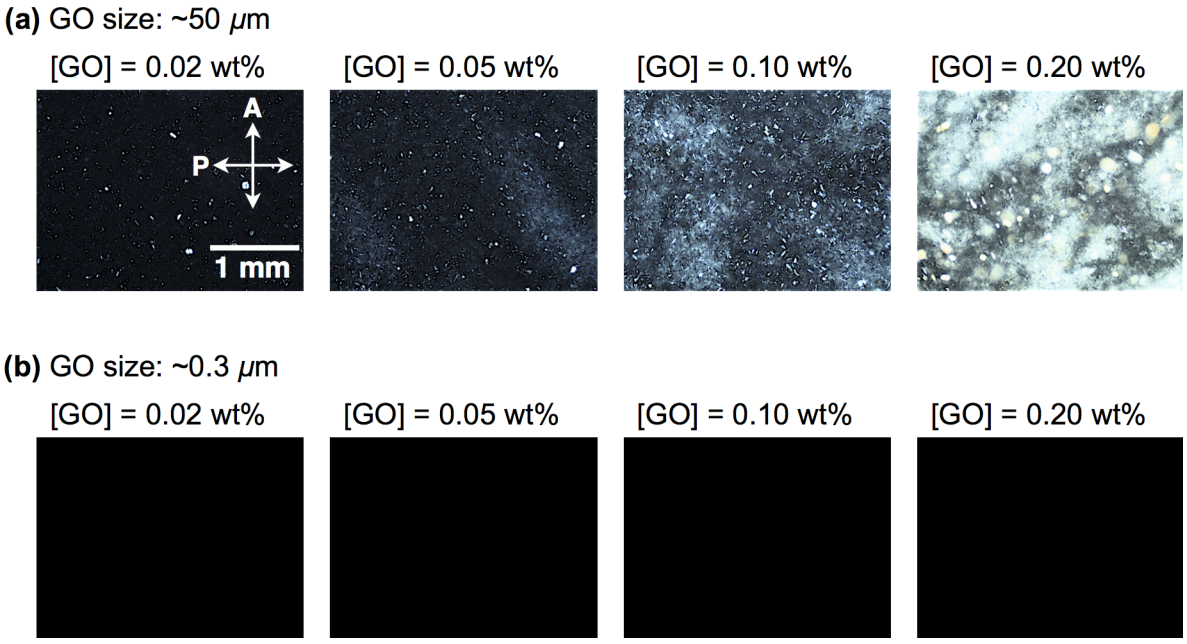

Figure S12. POM images of aqueous dispersions (in 1-mm cell) of GO with the averaged sizes of (a) ~50 and (b) ~0.3 μm. [GO] = (i) 0.02, (ii) 0.05, (iii) 0.10, and (iv) 0.20 wt%.

10. 2D SAXS Images of GO/RGO-Hybridized Hydrogels

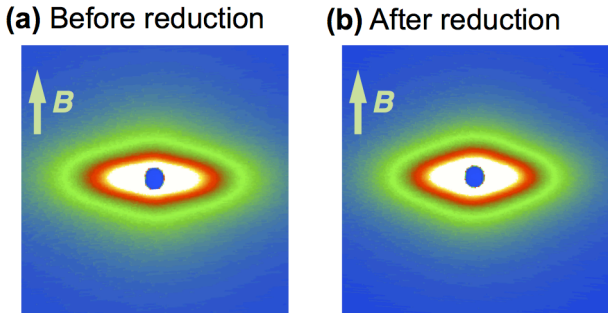

Figure S13. 2D-SAXS images of GO/RGO-hybridized hydrogels: (a) a GO-hybridized hydrogel (GO/monomer/crosslinker = 0.20/3.0/0.16 wt%, prepared in a 10-T magnetic field) and (b) a RCO-hybridized hydrogel prepared by the chemical reduction of GO in the GO-hybridized hydrogel. The hydrogels were exposed to an X-ray beam from the orthogonal direction to the magnetic field applied in the preparation of the GO-hybridized hydrogel.

11. POM Images of an RGO-Hybridized Hydrogel

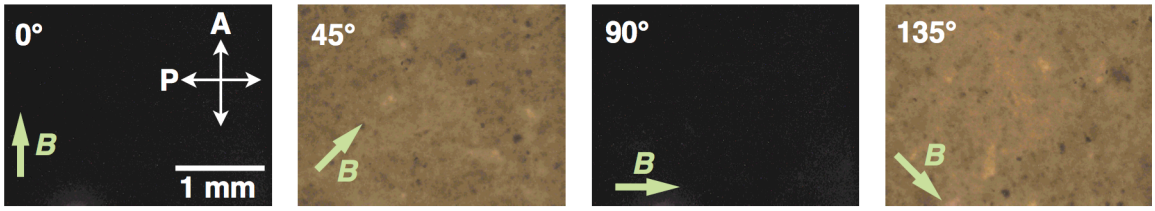

Figure S14. POM images of an RGO-hybridized hydrogel (1-mm thick) prepared by the chemical reduction of GO in a GO-hybridized hydrogel (GO/monomer/crosslinker = 0.20/3.0/0.16 wt%, prepared in a 10-T magnetic field). The images were obtained by varying the angle between the direction of the analyzer and that of the applied magnetic field (0°, 45°, 90°, and 135°).

12. Preparation of RGO-Hybridized Hydrogel by the Pre-Reduction Route

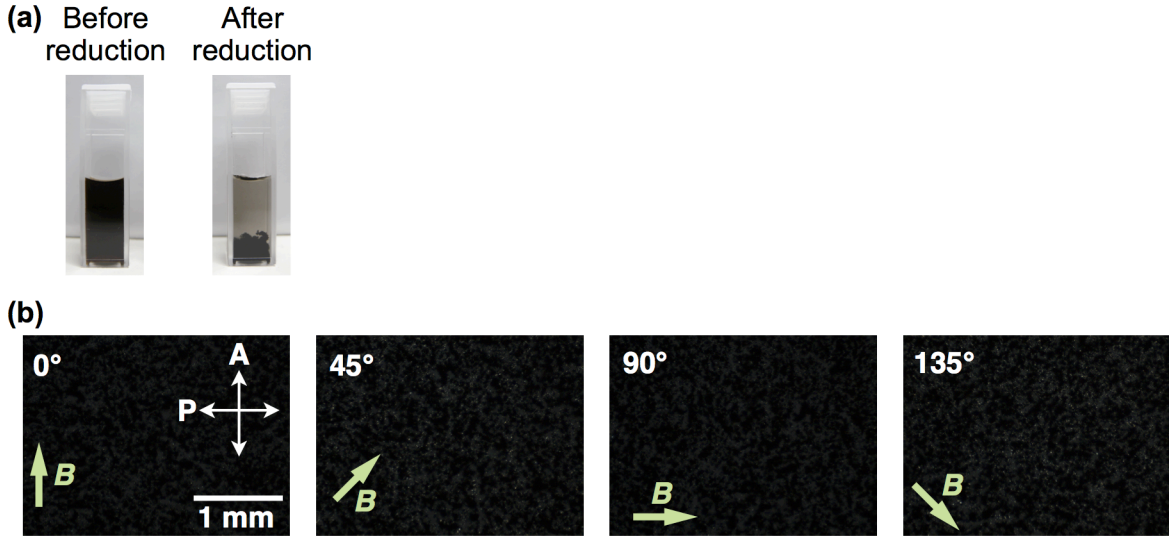

Figure S15. (a) Pictures of an aqueous mixture of GO ($[GO]_0$ = 0.20 wt%) before (left) and after (right) the treatment with reducing agents ($[KOH]_0$ = 1.6 M, $[HI]_0$ = 55%) at 20 °C. (b) POM images of an RGO-hybridized hydrogel (1-mm thick) prepared with the above mixture by in situ crosslinking polymerization of an acryl monomer (*N*,*N*-dimethylacrylamide, 3.0 wt%) and a crosslinker (*N*,*N*'-methylenebis(acrylamide), 0.16 wt%) in a 10-T magnetic field. The images were obtained by varying the angle between the direction of the analyzer and that of the applied magnetic field (0°, 45°, 90°, and 135°).

13. 2D-SAXS Images of RGO-Hybridized Organo- and Ionogels

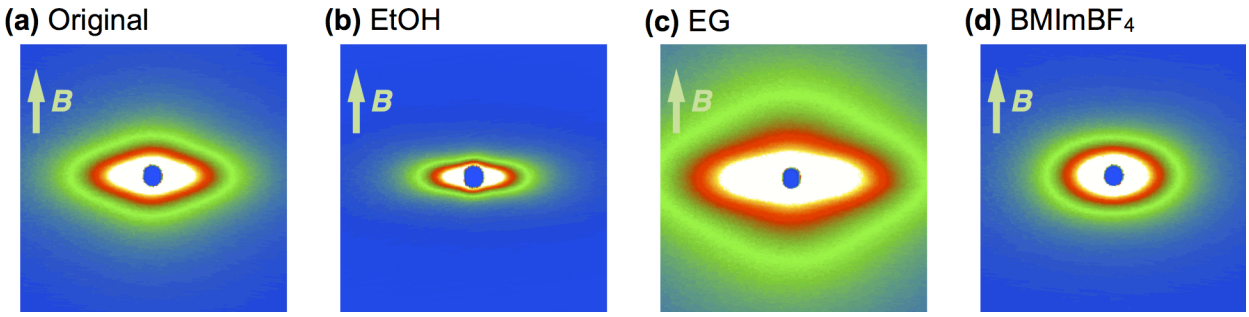

Figure S16. 2D-SAXS images of RGO-hybridized gels. An RGO-hybridized hydrogel was prepared by the chemical reduction of GO in a GO-hybridized hydrogel (GO/monomer/crosslinker = 0.20/3.0/0.16 wt%, prepared in a 10-T magnetic field). The RGO-hybridized hydrogel was immersed at 20 °C for 12 h three times in a fresh solvent (1,000 vol%): (a) original hydrogel and gels after immersion in (b) ethanol (EtOH), (c) ethylene glycol (EG), and (d) 1-butyl-4-methylimidazolium tetrafluoroborate ($BMImBF_4$). The gels were exposed to an X-ray beam from the orthogonal direction to the magnetic field applied in the preparation of the GO-hybridized hydrogel.

14. Characterization of GO-Hybridized Organo- and Ionogels

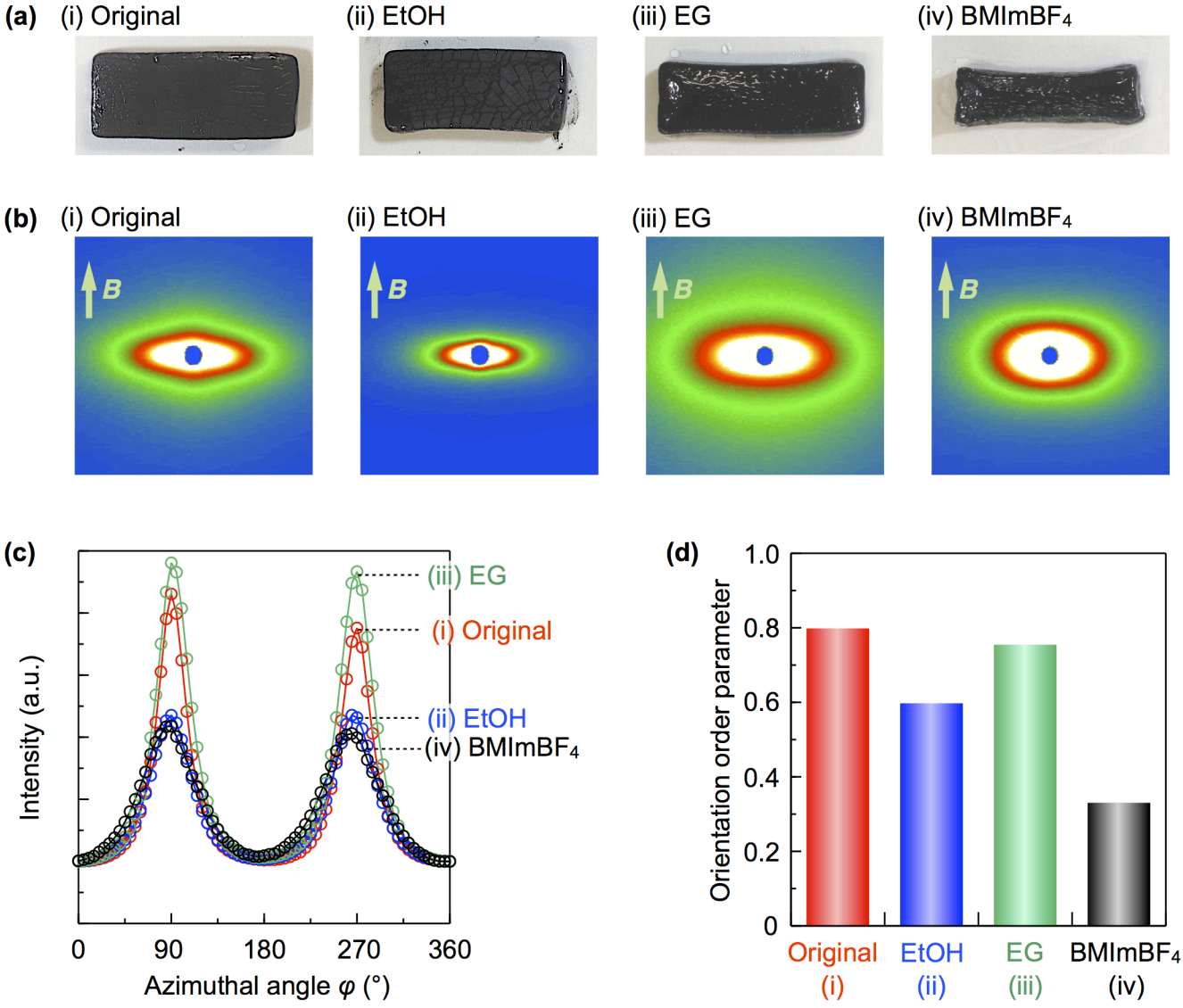

Figure S17. (a) Pictures (5-mm thick), (b) 2D-SAXS images, (c) azimuthal angle plots for the 2D-SAXS images, and (d) orientation order parameters of GO-hybridized gels. A GO-hybridized hydrogel (GO/monomer/crosslinker = 0.20/3.0/0.16 wt%, prepared in a 10-T magnetic field) was immersed m: (i) original hydrogel and gels after immersion in (ii) EtOH, (iii) EG, and (iv) $BMImBF_4$. In (b), the gels were exposed to an X-ray beam from the orthogonal direction to the magnetic field applied in the preparation of the GO-hybridized hydrogel.

15. Supporting References

S1. Feng, S.; Xiong, X.; Zhang, G.; Xia, N.; Chen, Y.; Wang, W. Hierarchical Structure in Oriented Fibers of a Dendronized Polymer. *Macromolecules* **2009**, *42*, 281–287.

S2. Nie, Y. J.; Huang, G. S.; Qu, L. L.; Wang, X.; Weng, G. S.; Wu, J. R. New Insights into Thermodynamic Description of Strain-Induced Crystallization of Peroxide Cross-Linked Natural Rubber Filled with Clay by Tube Model. *Polymer* **2011**, *52*, 3234–3242.

S3. Mitchell, G. R. In *Comprehensive Polymer Science*; Allen, G. and Bevington, J. C. Eds.; Pergamon Press: Oxford, 1989; Vol. 1.